JACS
JOURNAL OF THE AMERICAN CHEMICAL SOCIETY

Communication

pubs.acs.org/JACS

Tip-Induced Chemical Manipulation of Metal Porphyrins at a Liquid/Solid Interface

Min Li,[†,‡,∇] Duncan den Boer,[†,§,∇] Patrizia Iavicoli,[∥,#] Jinne Adisoejoso,[†] Hiroshi Uji-i,[†] Mark Van der Auweraer,[†] David B. Amabilino,*[,∥,⊥] Johannes A. A. W. Elemans,*[,§] and Steven De Feyter*[,†]

[†]Division of Molecular Imaging and Photonics, KU Leuven−University of Leuven, Celestijnenlaan 200-F, 3001 Leuven, Belgium

[‡]CAS Key Laboratory for Biomedical Effects of Nanomaterials and Nanosafety, Institute of High Energy Physics, Chinese Academy of Sciences, Beijing 100049, China

[§]Institute for Molecules and Materials, Radboud University Nijmegen, Heyendaalseweg 135, 6525 AJ Nijmegen, The Netherlands

[∥]Institut de Ciència de Materials de Barcelona (ICMAB-CSIC), Universitat Autónoma de Barcelona, Campus Universitari, 08193 Bellaterra, Catalonia, Spain

Supporting Information

ABSTRACT: Changing abruptly the potential between a scanning tunneling microscope tip and a graphite substrate induces "high-conductance" spots at the molecular level in a monolayer formed by a manganese chloride−porphyrin molecule. These events are attributed to the pulse-induced formation of μ-oxo-porphyrin dimers. The pulse voltage must pass a certain threshold for dimer formation, and pulse polarity determines the yield.

Scanning tunneling microscopy (STM) has proven to be a powerful technique to obtain spatial information at the atomic level and can be used to investigate dynamics and chemical phenomena on surfaces,[1−7] which is essential to explore the details of interfacial reaction processes involving single molecules.[8,9] The STM tips can also be used to initiate local reactions.[10−15] For instance, one-dimensional chain polymerization has been initiated by a voltage pulse applied to an STM tip during scanning.[1,16] It was also demonstrated that the polymerization of C_{60} into ring-like features can be induced.[17] The dissociation of molecules adsorbed on metal surfaces can be initiated as well, originating from a voltage pulse applied to the STM tip.[18,19] In addition, metal atomic manipulations on surfaces induced by a voltage pulse have been studied by STM, where the diffusion of the metal atoms was attributed to a lower activation energy caused by the voltage pulse.[20,21] Furthermore, voltage pulses can also provoke reversible single-molecule switching[22,23] and conformational changes of the absorbed molecules on surfaces.[24,25]

Most of these tip-induced reactions have been carried out under ultra-high-vacuum conditions. Liquid/solid interfaces are more complex, as reactions are not, by definition, confined to molecules adsorbed on the surface. While this could be considered a drawback, it also opens new possibilities for reactivity. Here, we report a localized STM-tip-induced reaction of a manganese chloride−porphyrin (Mn(III)-PP, Figure 1a) monolayer upon applying a voltage pulse at the liquid/solid interface between 1-octanoic acid and graphite, and reveal the importance of pulse height, polarity, and the presence of oxygen in the atmosphere on the outcome of the reaction.

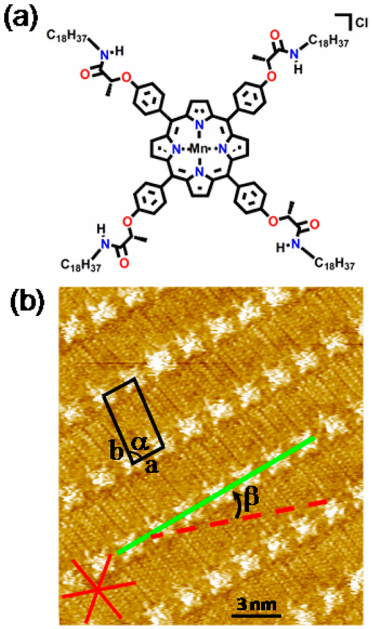

Figure 1. Molecular structure of Mn(III)-PP and its self-assembly pattern on graphite. (a) Chemical structure of Mn(III)-PP. (b) STM constant-current image (tunneling current I = 0.05 nA, sample bias V_s = −0.8 V) of a Mn(III)-PP monolayer self-assembled at a 1-octanoic acid/HOPG interface. Rows of porphyrin molecules do not run parallel to a main graphite axis but deviate by $\beta = -21 \pm 2°$ from this reference axis. Both the unit cell parameters (a = 1.9 ± 0.1 nm, b = 4.0 ± 0.1 nm, α = 83 ± 2°) and chiral expression are similar to those of the free base analogue of Mn(III)-PP.[26]

Mn(III)-porphyrins are well-known as catalysts in a wide range of oxidation reactions.[27] We have recently succeeded in detecting with STM different oxidation states of individual

Received: October 24, 2014
Published: November 24, 2014

   dx.doi.org/10.1021/ja510930z | J. Am. Chem. Soc. 2014, 136, 17418−17421

manganese porphyrins during their reaction with oxygen at a solid/liquid interface.[28] When a solution of Mn(III)-PP in 1-octanoic acid (10^{-5} M) was drop-cast at room temperature on the basal plane of highly oriented pyrolytic graphite (HOPG), a well-organized physisorbed monolayer was formed, as revealed by STM imaging in the liquid (Figure 1b). Similar to its free base porphyrin analogue, Mn(III)-PP arranges in rows in which the alkyl chains interdigitate into a densely packed structure.[26]

Upon applyication of several voltage pulses (pulse height P_s = −4.5 V, pulse width P_w = 100 μs) to the STM tip at different locations of the scanning area, many spots much brighter than those of the as-deposited compound are seen to emerge clearly in the monolayer (Figure 2a). The bright spots were observed

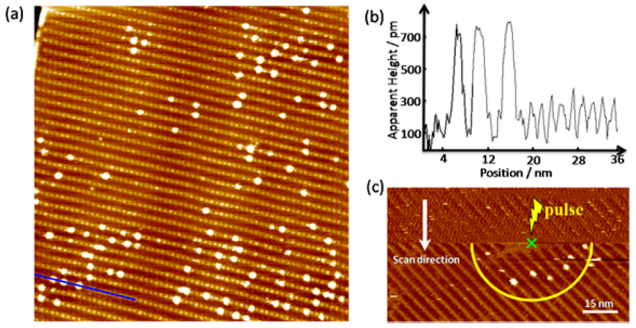

Figure 2. (a) STM image (108 nm × 108 nm) of a monolayer of Mn(III)-PP at the 1-octanoic acid/HOPG interface obtained after application of several pulses (P_s = −4.5 V). Many high-conductance spots appear. (b) Line profile along the blue line in (a). (c) STM image with bright spots, resulting from a single pulse. The pulse position is indicated by the green cross. The yellow line indicates the area affected, i.e., the area where bright spots are observed, after one single pulse. Scanning conditions: I = 0.05 nA, V_s = −0.8 V, P_s = −4.5 V, P_w = 100 μs, retract distance of the STM tip before pulsing = 15 Å.

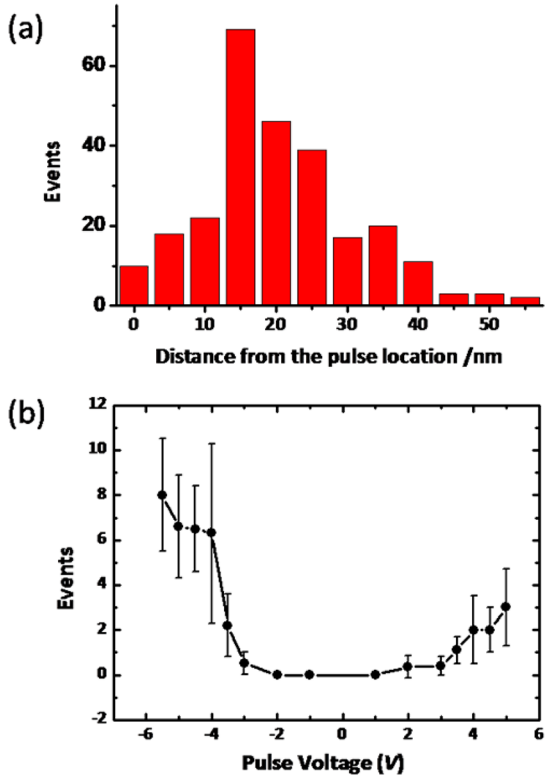

Figure 3. (a) Histogram of 48 single-pulse experiments (P_s = −4.5 V, 100 μs, 15 Å; V_s = −0.8 V; I = 0.05 nA), reflecting the number of bright spots as a function of the distance from the pulse location. (b) Yield of the bright spots as a function of the voltage of a single pulse to the sample, for V_s = −0.8 V. For histograms of the number of bright spots per pulse for the different pulse voltages, see SI, Figure S6 and Table S1.

exactly at the position of the Mn(III)-PP core in the monolayers (Figure 2a) and measured to be ∼0.8 nm in height (Figure 2b). One should note that the apparent height of the bright spot varies significantly between experiments (see Supporting Information (SI), Figure S1). In our previous work, the bright spot is measured to be 500 pm in height at a lower set-point, 10 pA.[28] In Figure 2c, the result of a single-pulse experiment is shown. The yellow line indicates the distribution of the bright spots in a local domain after one single negative substrate pulse (pulse voltage to the sample, P_s = −4.5 V, P_w = 100 μs, retracting the STM tip by 15 Å before pulsing). The pulse position is indicated by the green cross. The asymmetry of the tip geometry plays a role in the reaction. Specifically, it could give rise to an observed uneven distribution of product species because of the inhomogeneous electric field, as presented in SI, Figure S2c. Worthy of note is that, though the bright spot formation was the main focus in this work, species with a lower contrast[28] could still be observed, as shown in SI, Figure S3.

Figure 3a shows a histogram of single-pulse experiments (P_s = −4.5 V, P_w = 100 μs, substrate bias V_s = −0.8 V), reflecting the number of bright spots as a function of the distance from the pulse location. On average, ∼5−7 high-conductance spots are generated per pulse. This histogram is based on the data obtained in the first full scan (complete STM image) after the pulse. Note that the bright spots are demonstrated to be stable for several consecutive scans (SI, Figure S4). The spots were observed in a radial distribution surrounding the location of the pulse. Based on Figure 3a, ∼86% of the high-conductance spots appear within a radius of 30 nm from the pulse location (the total number of the collected bright spots is 259, of which 222 appeared within a radius of 30 nm). Note that the actual percentage could be higher, because the low yield of spots close to the pulse location (see, e.g., the bars between 0 and 10 nm in Figure 3a) is attributed not to a reduced efficiency but to an induced desorption of part of the monolayer in the direct vicinity of the pulse location (Figure S2).[4,29] Typically, the radius of the desorbed domain after one pulse is 13 ± 5 nm (Figure S2a), and it takes seconds to minutes to refill. Note that once (re)adsorbed, the degree of dynamics in the monolayer is very low (Figure S4), which is in line with observations for other porphyrin monolayers[30,31a] and is consistent with observations of kinetic control in layer assembly.[31] In a next series of experiments, we investigated the dependence of the appearance of the bright spots upon application of the pulse voltage in terms of pulse height and polarity. From the graph in Figure 3b, it is apparent that (1) at both pulse voltage polarities, bright spots are induced; (2) a larger magnitude of the pulse voltage, up to ±5.5 V, leads to more spots; (3) at both polarities, a threshold voltage (∼2−3 V) is observed before the spots appear; and (4) there is a yield dependency on the pulse voltage polarity, i.e., at negative substrate pulse voltages the yield is higher by a factor of ∼3.

The yield of the bright spots upon pulsing drops very fast with increasing the tip−sample distance. When the retract distance of the STM tip before pulsing is 1.5 nm, a significant

dx.doi.org/10.1021/ja510930z | J. Am. Chem. Soc. 2014, 136, 17418−17421

number of bright spots are induced. From 50 nm on, the yield drops dramatically to about one bright spot per pulse or no bright spots at all (SI, Figure S5).

Because Mn-porphyrins are known to show reactivity toward molecular oxygen, some pulse experiments were not carried out under ambient laboratory conditions but under an Ar atmosphere (see SI, Figure S7). A drastic decrease in the number of the bright spots appearing at a pulse voltage of −4.5 V was observed, with typically 0−2 remaining induced bright spots per pulse (see Figure S7b), which we attribute to a small remaining oxygen content in the solution.

The topographical signature in combination with the apparent height suggests a dimeric porphyrin structure.[28] Together with the observed oxygen dependence, we propose that the bright states correspond to μ-oxo dimers, which are well-known products of the reaction of Mn-porphyrin with oxygen.[32] We have recently detected these species during STM studies of Mn(III)-PP,[28] and by applying very low tunneling currents, the characteristic four-leaf clover structure of the top porphyrin could be sub-molecularly resolved (SI, Figure S8). Surface-bound μ-oxo Mn-porphyrin dimers have been proposed to form via a multistep reaction (Scheme 1), in

Scheme 1. Formation of a Mn-Porphyrin μ-Oxo Dimer via a Multistep Reaction

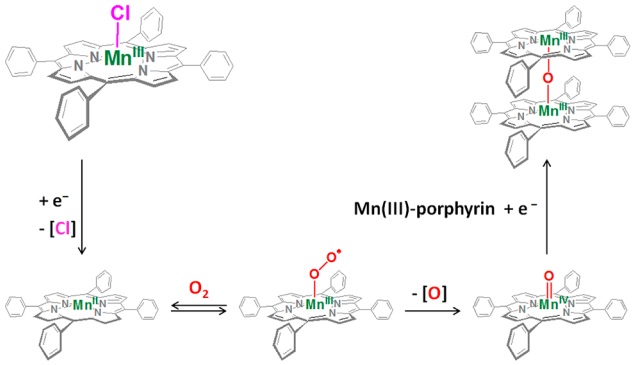

which first a surface-bound Mn(III)-porphyrin is reduced to a Mn(II)-porphyrin,[28,33] which subsequently reacts with oxygen to generate a Mn-dioxo species. After dissociation of the oxygen−oxygen bond, a reactive Mn(IV)-oxo intermediate is formed,[34] which can subsequently react with an additional Mn(III)-porphyrin. This reaction could happen from solution to form, upon the addition of an extra electron, the μ-oxo dimer if it is surface bound, or vice versa if it is a dissolved Mn(IV)-oxo species that reacts with an Mn(III)-porphyrin on the surface.

The application of a voltage pulse can explain the delivery of the two electrons and the second porphyrin needed for the formation of the Mn-porphyrin μ-oxo dimer products, as well as the specific locations of these formed dimers. Several factors can play important roles: (1) During the pulse, "hot electrons" are present in the tunneling current that might have sufficient energy to enable a reduction of Mn(III)-porphyrins at the surface, as well as in the solution.[35] However, as μ-oxo dimeric products have been observed as far as 50 nm from the location of the pulse (see Figure 3a), it is unlikely that the tunneling electrons are the sole cause of the reaction. Since the self-assembled monolayer is formed on graphite and not on a metal surface, the injection of hot carriers into the substrate[8,19] is unlikely. (2) An electric field has been found to change effective intermolecular potentials,[19] and this could change the energy landscape of a chemical reaction.[25] (3) The applied voltage during the pulse leads also to a high induced charge on the tip apex and a nearby surface. The electronic coupling between the molecules and the surface can be expected to be higher than with the tip. Therefore, electrons induced by a negative pulse on the surface will be more likely to reduce a Mn(III)-porphyrin than those electrons induced on the tip by a positive pulse, which could explain the higher yield at negative pulse voltages (Figure 3b). Furthermore, the difference between work function of the graphite surface (4.6 eV) and the Pt/Ir alloy tip (5.7 eV) also makes it more likely for the Mn(III)-PP molecules to obtain an electron from the graphite surface. (4) The pulse also leads to a very high inhomogeneous electric field near the tip apex, which may attract the polarizable Mn-porphyrins in solution, leading to a high local concentration.[36] This would explain the relatively high abundance of Mn-porphyrin μ-oxo dimers (and not single Mn-porphyrin oxo complexes) close to the location of the pulse. (5) At the pulse location, it would be no surprise if a lot of Mn(III)-to-Mn(II) reductions occur, and at the same time molecules are "blown away" from the surface into solution. Mn(II)-porphyrins are very reactive toward O_2. If then O−O splitting occurs (perhaps still because of the pulse), the resulting porphyrin Mn(IV)═O species may well land on another, remote porphyrin to form a μ-oxo dimer. (6) The reactive porphyrin intermediates, generated as a result of the pulse, apparently have faster reaction kinetics with porphyrins in the non-desorbed part of the layer than the re-adsorption kinetics at the desorption spot. In the non-desorbed domain, the exchange of adsorbed porphyrins with those in solution is limited (see Figure S4), and the observed μ-oxo Mn-porphyrin dimer products are therefore expected to be mostly formed on the surface. Close to the pulse location, however, desorption and re-adsorption of porphyrins play a prominent role. In the case that a reactive porphyrin intermediate reacts with a porphyrin in solution, the resulting μ-oxo Mn-porphyrin dimer product can either diffuse away or re-adsorb at the location of the pulse. Combined with the fact that a substantial amount of unreacted Mn(III)-porphyrins is also still present in solution, and competes for adsorption, the relative abundance of re-adsorbed μ-oxo Mn-porphyrin dimers on the surface is expected to be lower close to the pulse location than at the surrounding non-desorbed area (which is in line with the observations depicted in Figure 3a).

In summary, we have been able to induce a local chemical reaction on a surface by applying a pulse voltage with the STM tip. The yield dependence of the bright dots on the pulse voltage and pulse polarity was investigated thoroughly. Based on the results of the atmosphere-control experiments, we propose here that the bright dots are related to oxidation products of Mn(III)-PP, i.e., μ-oxo dimers, which is consistent with our previous study.[28] This work opens the way to manipulate reactions locally at the nanoscale, in particular at liquid/solid interfaces.

■ ASSOCIATED CONTENT

Supporting Information

Additional experimental details, STM images, and data analysis. This material is available free of charge via the Internet at http://pubs.acs.org.

dx.doi.org/10.1021/ja510930z | J. Am. Chem. Soc. 2014, 136, 17418−17421

AUTHOR INFORMATION

Corresponding Authors

david.amabilino@nottingham.ac.uk
j.elemans@science.ru.nl
steven.defeyter@chem.kuleuven.be

Present Addresses

[#]P.I.: European Commission Joint Research Centre, Via Enrico Fermi 2749, 21027 Ispra (VA), Italy
[⊥]D.B.A.: School of Chemistry, The University of Nottingham, Nottingham NG7 2RD, UK

Author Contributions

[▽]M.L. and D.d.B. contributed equally.

Notes

The authors declare no competing financial interest.

ACKNOWLEDGMENTS

J.A.A.W.E. and D.d.B. thank Nano*Lab* Nijmegen and the Council for the Chemical Sciences of The Netherlands Organisation for Scientific Research (CW-NWO) for a Vidi grant (700.58.423). J.A.A.W.E. thanks the European Research Council for an ERC Starting Grant (NANOCAT-259064) and the Dutch Ministry of Education, Culture and Science (Gravity program 024.001.035). S.D.F. thanks the Fund of Scientific Research Flanders (FWO), KU Leuven, for providing a GOA grant, and the Belgian Federal Science Policy Office (IAP 7/05). This research has also received funding from the European Research Council under the European Union's Seventh Framework Programme (FP7/2007-2013)/ERC Grant Agreement no. 340324. M.L. acknowledges funding from the National Natural Science Foundation of China (grant no. 21303208) and the National Basic Research Program (973 Program) of China (No. 2011CB933101).

REFERENCES

(1) Okawa, Y.; Aono, M. *Nature* **2001**, *409*, 683.
(2) Grill, L.; Dyer, M.; Lafferentz, L.; Persson, M.; Peters, M. V.; Hecht, S. *Nat. Nanotechnol.* **2007**, *2*, 687.
(3) Gimzewski, J. K.; Joachim, C. *Science* **1999**, *283*, 1683.
(4) Gaudioso, J.; Lee, H. J.; Ho, W. *J. Am. Chem. Soc.* **1999**, *121*, 8479.
(5) Lopinski, G. P.; Wayner, D. D. M.; Wolkow, R. A. *Nature* **2000**, *406*, 48.
(6) Heinz, R.; Stabel, A.; Rabe, J. P.; Wegner, G.; De Schryver, F. C.; Corens, D.; Dehaen, W.; Süling, C. *Angew. Chem., Int. Ed.* **1994**, *33*, 2080.
(7) Abdel-Mottaleb, M. M. S.; De Feyter, S.; Gesquière, A.; Sieffert, M.; Klapper, M.; Müllen, K.; De Schryver, F. C. *Nano Lett.* **2001**, *1*, 353.
(8) Maksymovych, P.; Sorescu, D. C.; Jordan, K. D.; Yates, J. T. *Science* **2008**, *322*, 1664.
(9) Ho, W. *J. Chem. Phys.* **2002**, *117*, 11033.
(10) Dujardin, G.; Walkup, R. E.; Avouris, P. *Science* **1992**, *255*, 1232.
(11) Stipe, B. C.; Rezaei, M. A.; Ho, W.; Gao, S.; Persson, M.; Lundqvist, B. I. *Phys. Rev. Lett.* **1997**, *78*, 4410.
(12) Ho, W. *Acc. Chem. Res.* **1998**, *31*, 567.
(13) Lee, H. J.; Ho, W. *Science* **1999**, *286*, 1719.
(14) Repp, J.; Meyer, G.; Paavilainen, S.; Olsson, F. E.; Persson, M. *Science* **2006**, *312*, 1196.
(15) Lastapis, M.; Martin, M.; Riedel, D.; Hellner, L.; Comtet, G.; Dujardin, G. *Science* **2005**, *308*, 1000.
(16) Miura, A.; De Feyter, S.; Abdel-Mottaleb, M. M. S.; Gesquière, A.; Grim, P. C. M.; Moessner, G.; Sieffert, M.; Klapper, M.; Müllen, K.; De Schryver, F. C. *Langmuir* **2003**, *19*, 6474.
(17) Nouchi, R.; Masunari, K.; Ohta, T.; Kubozono, Y.; Iwasa, Y. *Phys. Rev. Lett.* **2006**, *97*, 196101/1.
(18) Chen, L.; Li, H.; Wee, A. T. S. *ACS Nano* **2009**, *3*, 3684.
(19) Maksymovych, P.; Dougherty, D. B.; Zhu, X. Y.; Yates, J. T. *Phys. Rev. Lett.* **2007**, *99*, 016101/1.
(20) Tsong, T. T. *Phys. Rev. B* **1991**, *44*, 13703.
(21) Hasegawa, Y.; Avouris, P. *Science* **1992**, *258*, 1763.
(22) Huang, Y. L.; Lu, Y. H.; Niu, T. C.; Huang, H.; Kera, S.; Ueno, N.; Wee, A. T. S.; Chen, W. *Small* **2012**, *8*, 1423.
(23) Zhang, J. L.; Xu, J. L.; Niu, T. C.; Lu, Y. H.; Liu, L.; Chen, W. *J. Phys. Chem. C* **2014**, *118*, 1712.
(24) Boland, J. J. *Science* **1993**, *262*, 1703.
(25) Alemani, M.; Peters, M. V.; Hecht, S.; Rieder, K. H.; Moresco, F.; Grill, L. *J. Am. Chem. Soc.* **2006**, *128*, 14446.
(26) Linares, M.; Iavicoli, P.; Psychogyiopoulou, K.; Beljonne, D.; De Feyter, S.; Lazzaroni, R.; Amabilino, D. B. *Langmuir* **2008**, *24*, 9566. Note that a different reference axis is used.
(27) Meunier, B. *Chem. Rev.* **1992**, *92*, 1411.
(28) den Boer, D.; Li, M.; Habets, T.; Iavicoli, P.; Rowan, A. E.; Nolte, R. J. M.; Speller, S.; Amabilino, D. B.; De Feyter, S.; Elemans, J. A. A. W. *Nat. Chem.* **2013**, *5*, 621.
(29) Wang, C.; Bai, C. L.; Li, X. D.; Shang, G. Y.; Lee, I.; Wang, X. W.; Qiu, X. H.; Tian, F. *Appl. Phys. Lett.* **1996**, *69*, 348.
(30) Coenen, M. J. J.; Cremers, M.; den Boer, D.; van den Bruele, F. J.; Khoury, T.; Sintic, M.; Crossley, M. J.; van Enckevort, W. J. P.; Hendriksen, B. L. M.; Elemans, J. A. A. W.; Speller, S. *Chem. Commun.* **2011**, *47*, 9666.
(31) (a) Bhattarai, A.; Mazur, U.; Hipps, K. W. *J. Am. Chem. Soc.* **2014**, *136*, 2142. (b) Friesen, B. A.; Bhattarai, A.; Mazur, U.; Hipps, K. W. *J. Am. Chem. Soc.* **2012**, *134*, 14897.
(32) (a) Feiters, M. C.; Rowan, A. E.; Nolte, R. J. M. *Chem. Soc. Rev.* **2000**, *29*, 375. (b) Meunier, B. *Chem. Rev.* **1992**, *92*, 1411. (c) Lyons, J. E.; Ellis, P. E.; Myers, H. K. *J. Catal.* **1995**, *155*, 59.
(33) Hulsken, B.; Van Hameren, R.; Gerritsen, J. W.; Khoury, T.; Thordarson, P.; Crossley, M. J.; Rowan, A. E.; Nolte, R. J. M.; Elemans, J. A. A. W.; Speller, S. *Nat. Nanotechnol.* **2007**, *2*, 285.
(34) Tabushi, I. *Coord. Chem. Rev.* **1988**, *86*, 1.
(35) (a) Smejtek, P.; Silver, M. *J. Phys. Chem.* **1972**, *76*, 3890. (b) Čížek, M.; Horáček, J.; Allan, M.; Fabrikant, I. I.; Domcke, W. *J. Phys. B: At. Mol. Opt. Phys.* **2003**, *36*, 2837. (c) Sze, S. M.; Crowell, C. R.; Carey, G. P.; Labate, E. E. *J. Appl. Phys.* **1966**, *37*, 2690.
(36) (a) Fuchsel, G.; Klamroth, T.; Dokic, J.; Saalfrank, P. *J. Phys. Chem. B* **2006**, *110*, 1633736. (b) Ni, K.-K.; Ospelkaus, S.; Wang, D.; Quéméner, G.; Neyenhuis, B.; Miranda, M. H. G. D.; Bohn, J. L.; Ye, J.; Jin, D. S. *Nature* **2010**, *464*, 1324.